

Intermittency in the velocity distribution of heavy particles in turbulence

J. BEC^{1†}, L. BIFERALE², M. CENCINI³, A. S. LANOTTE⁴
AND F. TOSCHI^{5,6}

¹Université de Nice-Sophia Antipolis, CNRS, Observatoire de la Côte d'Azur, Laboratoire Cassiopée,
Bd. de l'Observatoire, 06300 Nice, France

²Department of Physics and INFN, University of Rome Tor Vergata, Via della Ricerca Scientifica 1,
00133 Rome, Italy

³INFM-CNR, SMC Dept. of Physics, Università ‘La Sapienza’, P.zza A. Moro 2, and ISC-CNR, Via dei
Taurini 19, 00185 Roma, Italy

⁴ISAC-CNR, Via Fosso del Cavaliere 100, 00133 Rome and INFN, Sez. Lecce, 73100 Lecce, Italy

⁵Department of Physics and Department of Mathematics and Computer Science, Eindhoven University
of Technology, 5600 MB Eindhoven, The Netherlands

⁶Istituto per le Applicazioni del Calcolo CNR, Viale del Policlinico 137, 00161 Roma, Italy

(INTERNATIONAL COLLABORATION FOR TURBULENCE RESEARCH)

(Received 25 June 2009; revised 9 December 2009; accepted 23 December 2009)

The statistics of velocity differences between pairs of heavy inertial point particles suspended in an incompressible turbulent flow is studied and found to be extremely intermittent. The problem is particularly relevant to the estimation of the efficiency of collisions among heavy particles in turbulence. We found that when particles are separated by distances within the dissipative subrange, the competition between regions with quiet regular velocity distributions and regions where very close particles have very different velocities (caustics) leads to a quasi bi-fractal behaviour of the particle velocity structure functions. Contrastingly, we show that for particles separated by inertial-range distances, the velocity-difference statistics can be characterized in terms of a local roughness exponent, which is a function of the scale-dependent particle Stokes number only. Results are obtained from high-resolution direct numerical simulations up to 2048^3 collocation points and with millions of particles for each Stokes number.

1. Introduction

Two effects have recently been singled out to explain the speed-up of collisions between small finite-size particles suspended in turbulent flows (see Sundaram & Collins 1997; Falkovich, Fouxon & Stepanov 2002; Shaw 2003). The first is *preferential concentration*, which is the development of strong inhomogeneities in their spatial distribution (see figure 1a) (Zhou, Wexler & Wang 1998, 2001; Reade & Collins 2000; Goto & Vassilicos 2008). The second is the formation of *fold caustics* (a phenomenon also called the *sling effect*), which results in high probabilities that very close particles exhibit large relative velocities (see figure 1b) (Bec *et al.* 2005; Wilkinson & Mehlig 2005; Wilkinson, Mehlig & Bezuglyy 2006; Falkovich & Pumir 2007; Olla 2008).

† Email address for correspondence: jeremie.bec@obs-nice.fr

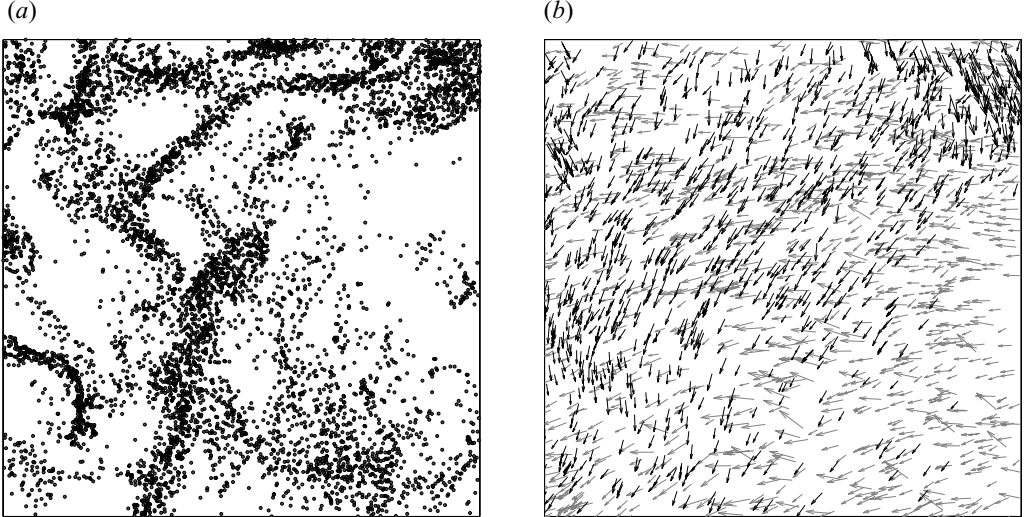


FIGURE 1. (a) Snapshot of the position of particles for $St = 2$ in a slice of size $5\eta \times 100\eta \times 100\eta$ for $Re_\lambda \approx 400$. (b) Particle velocity field in the same slice for a larger Stokes, $St = 20$, showing the existence of regions where particles have different velocities (highlighted by grey and black arrows, respectively).

Improving the collision kernels used in kinetic models for atmospheric physics, astrophysics and engineering requires quantifying precisely the individual contribution of these two effects and, in particular, to what extent turbulence might affect them, i.e. how they depend on the Taylor-scale Reynolds number Re_λ of the flow (see e.g. Derevyanko, Falkovich & Turitsyn 2008; Xue, Wang & Grabowski 2008).

We consider suspensions of small, heavy and dilute particles, neglecting gravity. As observed by Ayala *et al.* (2008) for dynamics of water droplets in warm clouds, gravitational settling is found to dominate the statistics of velocity differences between particles. However, this effect acts mainly between particles of different sizes that fall at different speeds. Present results could apply, for example, to early stage of cumulus cloud evolution during which the droplets are almost monodisperse and might play an important role in explaining the size spectral broadening observed in clouds.

We found two main results. First, we show for the first time that velocity differences between two particles enjoy a very intermittent distribution for separation scales inside the viscous dissipative range, with saturation of the scaling exponents for high-order moments of separations. Second, in the inertial range, velocity differences can be characterized in terms of a scale-dependent Stokes number, measuring the ratio between the particle response time and the eddy turnover time at the considered scale. Both results show the highly non-trivial statistics of heavy particle distribution and velocities in turbulent flows. Before detailing the results, we introduce the physical and the numerical set-up of our study.

We consider point particles that are simply dragged by viscous forces and each individual trajectory $\mathbf{X}(t)$ solves the equation:

$$\ddot{\mathbf{X}} = -\frac{1}{\tau} [\dot{\mathbf{X}} - \mathbf{u}(\mathbf{X}, t)], \quad (1.1)$$

where dots denote time derivatives, \mathbf{u} the fluid velocity field, solution of the incompressible Navier–Stokes equation and $\tau = a^2(2\rho_p + \rho_f)/(9\nu\rho_f)$ the particle

response time, also called Stokes time; where ρ_p and ρ_f are the particle and fluid densities, respectively, a is the particle radius and ν is the fluid kinematic viscosity (see Toschi & Bodenschatz 2009 for a recent review). The importance of inertia in the particle dynamics is quantified by the *Stokes number* $St = \tau/\tau_\eta$, where τ_η is the dissipative Kolmogorov time scale. Following Reade & Collins (2000), the collision rates between particles are evaluated using the ghost-particle approach, which assumes that particles can occupy any point of space independently of the positions of others. This approximation is valid in the asymptotics of very diluted suspensions, and has the advantage of relying on stationary dynamical statistics: the geometrical collision rate is then determined by the value at $r=2a$ of the *approaching rate* (see Bec *et al.* 2005):

$$\kappa(r; St) = -\langle |\dot{R}| \mid R=r \text{ and } \dot{R} \leq 0 \rangle p_2(r; St). \quad (1.2)$$

Here R denotes the distance between two particles with Stokes number St , and $p_2(r; St)$ is the probability density to find two particles at separation r . The average is performed over time and particle pairs, with the condition to be separated by a distance r and to approach each other. Clearly the behaviour of $\kappa(r; St)$ prescribes the dependence of the collision rate upon the particle attributes (size and mass density contrast). Caustics and preferential concentration (figure 1) intricately appear in (1.2) affecting the conditional average of the velocity difference \dot{R} and the r -dependence of p_2 , respectively. In the dissipative range ($r \ll \eta$),

$$p_2(r; St) \propto r^{D_2(St)-1},$$

where $D_2(St) \in [0, d]$ is the *correlation dimension* of the particle distribution in d dimensions (see for instance Grassberger 1983) and non-trivially depends on the Stokes number as shown by Bec *et al.* (2007). We remark that in the literature (see e.g. Reade & Collins 2000) the contribution of preferential concentration to collisions is often accounted in terms of the radial distribution function $g(r)$, which can be expressed as the ratio between the actual number of particles inside an infinitesimally thin shell of radius r centred on a given particle and the number that would be expected if the particles were uniformly distributed. The enhancement of the collision probability due to preferential concentration is typically associated to the divergence of $g(r)$ for $r \ll \eta$ (see Reade & Collins 2000; Zhou, Wexler & Wang 2001). It is not difficult to see that the probability density $p_2(r; St)$ in (1.2) is straightforwardly related to the radial distribution function. In particular, the small-scale behaviour of the radial distribution function is linked to that of p_2 , and one has that $g(r) \sim r^{D_2(St)-d}$. Therefore, for particles uniformly distributed, $D_2(St)=d$, so that $g(r) \sim \mathcal{O}(1)$. On the contrary, when $D_2(St) < d$, the signature of particle clustering, $g(r)$ diverges as $r \rightarrow 0$.

We focus here on the velocity contribution to the approaching rate by studying the behaviour as a function of the separation r of the longitudinal particle velocity structure functions

$$S_p(r; St) = \langle |\dot{R}|^p \mid R=r \rangle. \quad (1.3)$$

The choice of defining structure functions with absolute values is motivated by the definition of the collision kernel (via the approaching rate). When focusing on the behaviour of $\kappa(r)$ as a function of the separation r , scaling properties are not affected when performing averages over positive or negative velocities. Indeed, similarly to fluid velocity increments, an asymmetry in the distribution of velocity difference is observed; however, we checked that such a skewness does not affect the behaviour of moments as a function of the spatial scale. For this reason, one can therefore estimate: $\kappa(r) \propto r^{D_2(St)-1} S_1(r; St)$ (see Bec *et al.* 2005). Evaluating $S_p(r; St)$

	<i>N</i>	<i>Re</i> _λ	<i>η</i>	<i>dx</i>	<i>ε</i>	<i>ν</i>	<i>τ</i> _η	<i>dt</i>
Run A	512	185	1×10^{-2}	1×10^{-2}	0.9	2×10^{-3}	4.7×10^{-2}	4×10^{-4}
Run B	2048	400	3×10^{-3}	3×10^{-3}	0.9	3.5×10^{-4}	2×10^{-2}	1.2×10^{-4}

TABLE 1. Eulerian and Lagrangian parameters for the two runs analysed in the text. *N*: number of grid points per spatial direction; *Re*_λ: Taylor-scale Reynolds number; *η*: Kolmogorov dissipative scale; *dx*: grid spacing; $\tau_\eta = \sqrt{\nu/\epsilon}$: Kolmogorov dissipative time scale, *ε*: energy dissipation; *ν*: kinematic viscosity; *dt*: temporal discretization. Total number of particle for each Stokes value is 7.5×10^6 for run A and $\sim 10^8$ for run B. The Navier–Stokes equations are solved on a cubic grid of size *N*³ with periodic boundary conditions. Energy is injected by keeping constant the spectral content of the two smallest wavenumber shells (Chen *et al.* 1993). The viscosity is chosen so to have a Kolmogorov length scale $\eta \approx dx$. This conservative choice yields to Reynolds numbers smaller than other direct numerical simulations at comparable resolution (see e.g. Gotoh, Fukayama & Nakano 2002; Yeung, Pope & Sawford 2006; Ishihara, Gotoh & Kaneda 2009). On the other hand, it ensures a good resolution of the small-scale velocity dynamics. We use a fully de-aliased pseudo-spectral algorithm with second-order Adams–Bashforth time-stepping (for details see Bec *et al.* 2006). Particle dynamics is evolved with a time steps from 10 to 1000 times smaller than the Stokes time, leading to an accurate resolution of the particle trajectories. Tri-linear interpolation is used to determine the value of the velocity field at the particle position. The high spatial Eulerian resolution ensure a smooth differentiable velocity field. Some raw data of particle trajectories are freely available from the iCFDdatabase (<http://cfd.cineca.it>).

for values of *p* different from 1, besides providing a more complete characterization of the velocity statistics, allows one to account also for fluctuations of the local approaching rate, which can vary significantly from place to place in the flow. High-order statistics give crucial information on the mechanisms for such fluctuations and are thus a pre-requisite for determining the validity of mean-field kinetic models used in application fields. In the limit of small inertia, the particle dynamics approaches that of tracers and consequently the velocity difference \dot{R} is essentially coincident with the fluid longitudinal increment over a separation *R*. Conversely, when $St \rightarrow \infty$, particles move ballistically in the flow with uncorrelated velocities and the structure functions $S_p(r; St)$ become independent of *r*. For intermediate values of the Stokes number, one expects a non-trivial behaviour of S_p as a function of *r* and *St*. Data analysed in this study come from direct numerical simulations up to $Re_\lambda \approx 400$ (see table 1 for details). Figure 2 shows the behaviour of the second-order structure function $S_2(r; St)$ for two different values of the carrier flow Reynolds number. One distinguishes different regimes, depending whether *r* is within the dissipative or inertial range of the turbulent carrier flow. While the dissipative-range behaviour directly relates to inter-particle collisions, the inertial-range behaviour has important implications in general on the relative dispersion of particles in turbulent flow as shown by Bec *et al.* (2009), and for pollution models in particular. In the sequel we investigate these two regimes separately.

2. Dissipative range

In the dissipative range, the structure functions display a power-law behaviour

$$S_p(r; St) \propto r^{\xi_p(St)}.$$

The two asymptotics of weak and strong inertia imply that $\xi_p(St) \simeq p$ for $St \ll 1$ and $\xi_p(St) \rightarrow 0$ for $St \rightarrow \infty$. For intermediate values of the Stokes number, $p \mapsto \xi_p(St)$ is

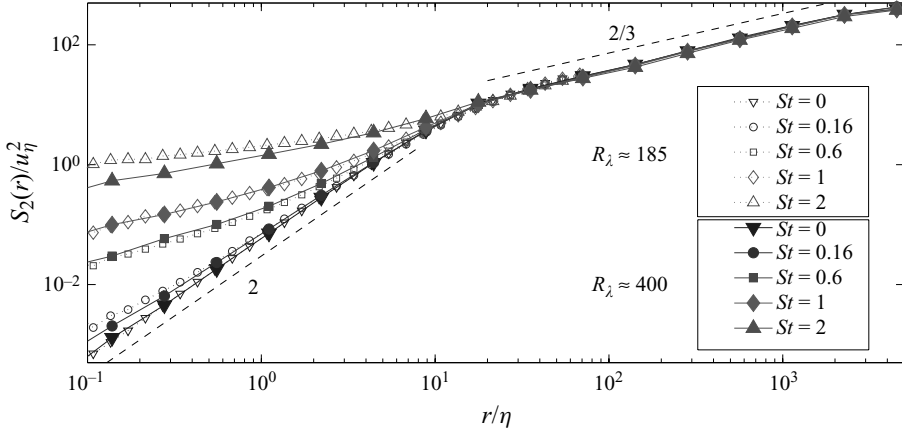


FIGURE 2. Second-order longitudinal velocity structure function for particles with various Stokes numbers and for two Reynolds numbers. Velocity increments are normalized with the fluid velocity at the Kolmogorov scale. The straight dashed lines correspond to the expected smooth scaling in the dissipative range, $\sim r^2$, and the expected Kolmogorov scaling in the inertial range, $\sim r^{2/3}$.

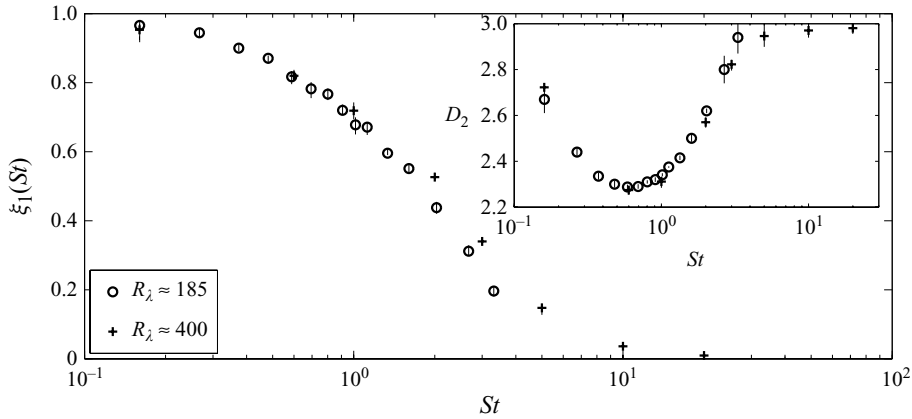


FIGURE 3. Dissipative-range scaling exponent, $\xi_1(St)$, versus the Stokes number St for two values of Re_λ . Inset: correlation dimension $D_2(St)$ as a function of St .

a convex function of the order p with values in $[0, p]$. Figure 3 shows the first-order exponent $\xi_1(St)$ as a function of the Stokes number. One can clearly observe that for $St = O(1)$, the exponent $\xi_1(St)$ takes non-trivial values spanning the whole interval $[0, 1]$. The dependence of the exponent upon Re_λ in the range spanned by our two simulations is very weak, if any.

At first glance the continuous variation of the exponent $\xi_1(St)$ from 1 to 0 at increasing St seems inconsistent with a naive picture of the role of caustics in velocity statistics. Fold caustics are a part of catastrophe theory (Arnold, Shandarin & Zel'dovich 1982); they occur when fast particles catch up with slower ones to create regions where particles with different velocities can be found at the same spatial location as seen in figure 1(b). If particles conserve their velocity and move ballistically, such caustics will extend over the whole domain; whence the analogy with caustics formed by light rays as detailed in Falkovich *et al.* (2002), Wilkinson & Mehligh (2005)

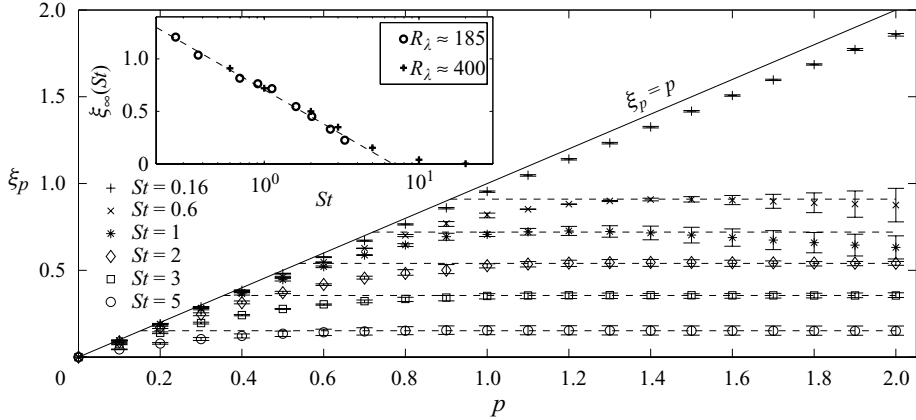


FIGURE 4. Scaling exponents $\xi_p(St)$ of the particle velocity structure functions $S_p(r)$ for various St and $Re_\lambda \approx 400$. Inset: saturation exponents $\xi_\infty(St)$ as a function of St for two values of Re_λ ; the dashed line represents a fit of the form $\propto \ln(7/St)$. Exponents are obtained by measuring the mean logarithmic derivative of $S_p(r)$ in $0.2 \leq (r/\eta) \leq 2$; errors correspond to the largest deviations observed in the fitting range. Moments of higher orders (not represented here to lighten the figure) were also computed; their behaviour confirms saturation of the exponents to a limiting finite value.

and Wilkinson *et al.* (2006). The typical velocity difference between two particles becomes independent of their distance, meaning that structure functions tend to a constant as $r \rightarrow 0$, and thus $\xi_p(St) = 0$, for any value of p . However, there are two clear reasons why this continuous-field picture may fail. First, because of their dissipative dynamics, particles concentrate on dynamical attractors in the position-velocity phase space (Bec *et al.* 2005). Such sets are fractal and correlated with the fluid and lead to the formation of caustics of various strength with non-trivial probabilities. Second, as the particle velocity relaxes to the fluid velocity, the spatio-temporal extent of such caustics may also have complex statistical properties.

To better quantify the contribution from caustics, we extend our investigation to the particle velocity scaling exponents in the dissipative range $\xi_p(St)$ with orders p other than 1, shown in figure 4 for various values of the Stokes number. At low orders, the exponents are almost tangent to the line $\xi_p(St) = p$ while, at large orders, they saturate to an asymptotic value $\xi_\infty(St)$, monotonically decreasing with St as shown in the inset. The crossover between these two regimes shifts to low orders when increasing the Stokes number, leading to a less and less sharp transition. Numerical data suggests for the limiting saturation exponent:

$$\left. \begin{aligned} \xi_\infty(St) &\propto \ln(7/St) && \text{for } St \lesssim 7, \\ \xi_\infty(St) &\simeq 0 && \text{for } St \gtrsim 7. \end{aligned} \right\} \quad (2.1)$$

Let us notice that critical Stokes number value for which $\xi_\infty \approx 0$, i.e. $St^* = 7$, is very close to that for which $D_2(St) \approx 3$ (see inset of figure 3). As discussed by Derevyanko *et al.* (2007) a saturation of $D_2(St)$ to the space dimension is indeed expected for St values at which caustics become dominating. In this respect, we also notice that the saturation exponent $\xi_\infty(St)$ can be interpreted as the codimension of large fold caustics associated to order-unity velocity jumps. Indeed, such caustics contribute to the structure function $S_p(r; St)$ a term of the form $V_p P(r)$ where V_p is the p th-order moment of the velocity difference inside the caustics and $P(r)$ is the probability

of having such a caustic present in a box of size r . The saturation of the scaling exponents suggests that $P(r) \propto r^{\xi_\infty(St)}$, so that $D^{(c)} \equiv 3 - \xi_\infty(St)$ is the (statistical) Hausdorff dimension of the set of caustics.

At smaller orders, the statistics is dominated by other events for which one can figure out two conceivable scenarios. A first possibility is that caustics distribution spans all possible sizes with non-trivial codimensions, i.e. is a multi-fractal. In this case they affect all orders and give rise to multi-scaling and to a non-trivial behaviour of the exponents $\xi_p(St)$ as a function of p , before the saturation (Celani *et al.* 2000). The alternative possibility is that the caustics are randomly distributed with a typical size and dominate the velocity statistics at large moments only, while small orders are controlled by the smooth regions of the particle velocity. In that case the structure function would display a bi-fractal behaviour similar to that present in random solutions to the Burgers equation (see e.g. Bec & Khanin 2007), namely

$$\left. \begin{array}{ll} \xi_p(St) = p & \text{if } p \leq \xi_\infty(St), \\ \xi_p(St) = \xi_\infty(St) & \text{if } p \geq \xi_\infty(St). \end{array} \right\} \quad (2.2)$$

As seen from figure 4, the measured exponents are very close to the bi-fractal behaviour. The observed deviations could be due to a real small multi-fractal component or to artifacts due to the presence of subleading terms or logarithmic corrections as shown by Biferale *et al.* (2004) and Mitra *et al.* (2005). Note that deviations from a bi-fractal behaviour seem very strong at large Stokes numbers, suggesting a softer distinction between smooth regions and caustics. However, the low values of the exponents in this asymptotics make even more difficult the estimation of subleading terms.

Numerical observations give strong evidence in favour of a saturation of the scaling exponents ξ_p at large orders. This suggests that caustics, while randomly distributed in space, have a typical velocity amplitude, which is entailed in the finiteness of the moments V_p introduced above. This ‘size of caustics’ depends of course on particle inertia, and thus on the Stokes number. Such a dependence is not visible when investigating the exponents ξ_p as a function of St , but can however be estimated through the asymptotics of weak and strong particle inertia. When $St \ll 1$, the relaxation of particles dynamics is so fast that caustics never develop except at locations where the fluid velocity gradient takes extreme values, thus leading to large velocity differences. Conversely, when $St \gg 1$, caustics fill the whole space but, as shown in Abrahamson (1975), particles individual velocities decrease as $St^{-1/2}$ and caustics amplitude becomes very small. The contribution of caustics amplitude to the approaching rate thus acts to compensate the size effect observed in the ξ_1 dependence on St . This implies that for a fixed (large) density ratio ρ_p/ρ_f there exists an optimal particle size a such that $(a/\eta)^2 = \mathcal{O}(\rho_f/\rho_p)$ (i.e. $St = \mathcal{O}(1)$), for which the monodisperse collision rate attains a maximum.

3. Inertial range

We finally turn to the behaviour of the velocity structure function for separations within the inertial range of turbulence, i.e. for $\eta \ll r \ll L$. As seen from figure 2, particle velocity structure functions recover the fluid ones when r becomes very large. Indeed as r increases the associated eddy turnover time grows as $r^{2/3}$ (where we used the Kolmogorov 1941 scaling (K41)) so that the effective strength of inertia reduces. Similarly to random self-similar carrier flows (see Bec *et al.* 2008), this effect can be

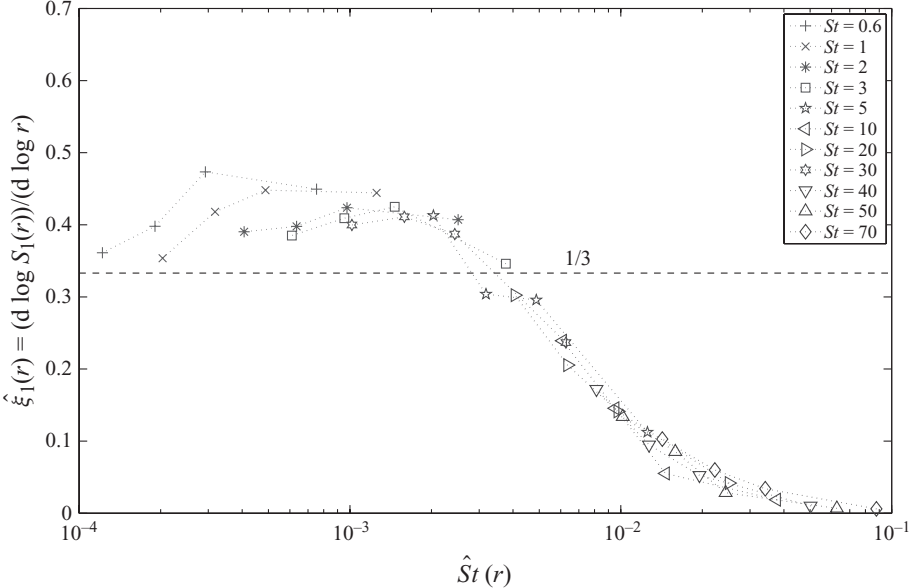


FIGURE 5. First-order local exponent $\hat{\xi}_1(r)$ as a function of the local Stokes number $\hat{St}(r)$ for $Re_\lambda \approx 400$. The horizontal dashed line represents tracers K41 expectation.

put on a quantitative ground in terms of a scale-dependent Stokes number,

$$\hat{St}(r) = \tau / (\varepsilon^{1/3} r^{2/3}), \quad (3.1)$$

defined as the ratio between the particle response time and the turnover time associated to the scale r , where ε denotes the mean dissipation rate of kinetic energy. We check whether the local scaling exponent

$$\hat{\xi}_p(r; \tau) \equiv (d \ln S_p(r; St)) / (d \ln r)$$

does depend on $\hat{St}(r)$ only, as observed in random self-similar flows by Bec *et al.* (2008). Figure 5 shows a good collapse of the values of $\hat{\xi}_1(r, \tau)$ associated to various τ and of r , once represented as a function of $\hat{St}(r)$. Moreover, the curve $\hat{\xi}_1(\hat{St}(r))$ has a shape qualitatively very similar to that of $\xi_1(St)$ observed in the dissipative range and shown in figure 3, this fact is relevant to heavy particle dispersion in turbulent flows (see e.g. Bec *et al.* 2009). Let us stress that data corresponding to small $\hat{St}(r)$ in figure 5 show deviations from the K41 scaling that are similar to those expected for tracers-like statistics.

4. Concluding remarks

To summarize, we have presented high-resolution direct numerical simulations of heavy particles evolution in homogeneous isotropic turbulence. We have studied both small-scales and inertial-range distribution of velocity differences between two particles; the former being relevant to the development of models for the collision kernel. We have found strong evidences of a highly intermittent distribution of caustics, leading to a quasi bi-fractal law for the scaling exponents of moments of velocity increments. The inertial-range statistics is governed by a *scale-dependent*

Stokes number, built in terms of the particle response time and of the scale-dependent eddy turn over time of the underlying flow. Both results may be crucial for a correct modelling of particle-particle interactions in real flows. In particular, the strong intermittency shown by the velocity increments in the viscous subrange suggests the importance of including fluctuations in the modelling of the collision kernel for large Stokes numbers.

We have estimated here collision rates in the framework of the ‘ghost particles’ approximation. This means that we let particle overlap whenever they reach a distance smaller than the sum of their radii. This assumption pertains to the asymptotics of very dilute suspensions, where the typical time between two successive collisions of a given particle is much longer than the relaxation time of its dynamics towards a statistically stationary regime. This approach has the advantage that all results discussed here are independent of the particle radii (except, of course, through the Stokes number), of the particle number density and of the type of collisions they experience. The motivation of studying such an asymptotic regime is to highlight universal mechanisms that are responsible for an increase of collisions rates due to particle inertia.

Finally, it is worth stressing that up to now, the design of efficient and realistic two-fluid models has been slowed down by the intricate behaviour of particle velocities that was studied in details here. The observed intermittency explains the difficulty of projecting the particle phase-space dynamics in order to construct a synthetic velocity field that advects the particles. Actually such concerns extend to the study of conditional distributions or the reduction of dimensionality in a much broader range of dissipative dynamical systems.

This study benefited from fruitful discussions with L. Collins, G. Falkovich, B. Mehlig, L.-P. Wang and M. Wilkinson. J. Bec and A. Lanotte acknowledge support from NSF under grant No. PHY05_51164 for their stay at the Kavli Institute for Theoretical Physics in the framework of the 2008 ‘Physics of Climate Change’ program. Part of this work was supported by ANR under grant No. BLAN07-1_192604. Simulations were performed at CASPUR and CINECA (Italy), and in the framework of the DEISA Extreme Computing Initiative supported by the DEISA Consortium (cofunded by the EU, FP6 project 508830).

REFERENCES

- ABRAHAMSON, J. 1975 Collision rates of small particles in a vigorously turbulent fluid. *Chem. Engng Sci.* **30**, 1371–1379.
- ARNOLD, V. I., SHANDARIN, S. F. & ZEL'DOVICH, YA. B. 1982 The large scale structure of the universe I. General properties. One-and two-dimensional models. *Geophys. Astrophys. Fluid Dyn.* **20**, 111.
- AYALA, O., ROSA, B., WANG, L.-P. & GRABOWSKI, W. W. 2008 Effects of turbulence on the geometric collision rate of sedimenting droplets. Part 1. Results from direct numerical simulation. *New J. Phys.* **10**, 075015.
- BEC, J., BIFERALE, L., BOFFETTA, G., CELANI, A., CENCINI, M., LANOTTE, A. S., MUSACCHIO, S. & TOSCHI, F. 2006 Acceleration statistics of heavy particles in turbulence. *J. Fluid Mech.* **550**, 349.
- BEC, J., BIFERALE, L., BOFFETTA, G., CENCINI, M., LANOTTE, A. S., MUSACCHIO, S. & TOSCHI, F. 2007 Heavy particle concentration in turbulence at dissipative and inertial scales. *Phys. Rev. Lett.* **98**, 084502.
- BEC, J., BIFERALE, L., LANOTTE, A. S., SCAGLIARINI, A. & TOSCHI, F. 2010. Turbulent pair dispersion of inertial particles. *J. Fluid Mech.* (in press).

- BEC, J., CELANI, A., CENCINI, M. & MUSACCHIO, S. 2005 Clustering and collisions of heavy particles in random smooth flows. *Phys. Fluids* **17**, 073301.
- BEC, J., CENCINI, M., HILLERBRAND, R. & TURITSYN, K. 2008 Stochastic suspensions of heavy particles. *Physica D* **237**, 2037.
- BEC, J. & KHANIN, K. 2007 Burgers turbulence. *Phys. Rep.* **447**, 1.
- BIFERALE, L., CENCINI, M., LANOTTE, A. S. & SBRAGAGLIA, M. 2004 Anomalous scaling and universality in hydrodynamic systems with power-law forcing. *New J. Phys.* **6**, 37.
- CELANI, A., LANOTTE, A. S., MAZZINO, A. & VERGASSOLA, M. 2000 Universality and saturation of intermittency in passive scalar turbulence. *Phys. Rev. Lett.* **84**, 2385.
- CHEN, S., DOOLEN, G. D., KRAICHNAN, R. H. & SHE, Z.-S. 1993 On statistical correlations between velocity increments and locally averaged dissipation in homogeneous turbulence. *Phys. Fluids A* **5**, 458.
- DEREVYANKO, S., FALKOVICH, G. & TURITSYN, S. 2008 Evolution of non-uniformly seeded warm clouds in idealized turbulent conditions. *New J. Phys.* **10**, 075019.
- DEREVYANKO, S., FALKOVICH, G., TURITSYN, K. & TURITSYN, S. 2007 Explosive growth of inhomogeneities in the distribution of droplets in a turbulent air. *J. Turbul.* **8**, 1.
- FALKOVICH, G., FOUXON, A. & STEPANOV, M. 2002 Acceleration of rain initiation by cloud turbulence. *Nature* **419**, 151.
- FALKOVICH, G. & PUMIR, A. 2007 Sling effect in collisions of water droplets in turbulent clouds. *J. Atmos. Sci.* **64**, 4497.
- GOTO, S. & VASSILICOS, J.-C. 2008 Sweep-stick mechanism of heavy particle clustering in fluid turbulence. *Phys. Rev. Lett.* **100**, 054503.
- GOTOH, T., FUKAYAMA, D. & NAKANO, T. 2002 Velocity field statistics in homogeneous steady turbulence obtained using a high-resolution direct numerical simulations. *Phys. Fluids* **14**, 1065.
- GRASSBERGER, P. 1983 Generalized dimensions of strange attractors. *Phys. Lett. A* **97**, 227.
- ISHIHARA, T., GOTOH, T. & KANEDA, Y. 2009 Study of high-Reynolds number isotropic turbulence by direct numerical simulation. *Annu. Rev. Fluid Mech.* **41** 165.
- MITRA, D., BEC, J., PANDIT, R. & FRISCH, U. 2005 Is multiscaling an artifact in the stochastically forced Burgers equation? *Phys. Rev. Lett.* **94**, 194501.
- OLLA, P. 2008 Clustering and collision of inertial particles in random velocity fields. *Phys. Rev. E* **77**, 065301.
- READE, W. C. & COLLINS, L. R. 2000 A numerical study of the particle size distribution of an aerosol undergoing turbulent coagulation. *Phys. Fluids* **12**, 2530.
- SHAW, R. A. 2003. Particle-turbulence interactions in atmospheric clouds. *Annu. Rev. Fluid Mech.* **35**, 183.
- SUNDARAM, S. & COLLINS, L. R. 1997 Collision statistics in an isotropic particle-laden turbulent suspension. Part 1. Direct numerical simulations. *J. Fluid Mech.* **335**, 75.
- TOSCHI, F. & BODENSCHATZ, E. 2009 Lagrangian properties of particles in turbulence. *Annu. Rev. Fluid Mech.* **41**, 375.
- WILKINSON, M. & MEHLIG, B. 2005 Caustics in turbulent aerosols. *Europhys. Lett.* **71**, 186.
- WILKINSON, M., MEHLIG, B. & BEZUGLYY, V. 2006 Caustic activation of rain showers. *Phys. Rev. Lett.* **97**, 048501.
- XUE, Y., WANG, L.-P. & GRABOWSKI, W. 2008 Growth of cloud droplets by turbulent collision-coalescence. *J. Atmos. Sci.* **65**, 331.
- YEUNG, P. K., POPE, S. B. & SAWFORD, B. L. 2006 Reynolds number dependence of Lagrangian statistics in large numerical simulations of isotropic turbulence. *J. Turbul.* **7**, N58.
- ZHOU, Y., WEXLER, A. S. & WANG, L.-P. 1998 On the collision rate of small particles in isotropic turbulence. II. Finite inertia case. *Phys. Fluids* **10**, 1206.
- ZHOU, Y., WEXLER, A. & WANG, L.-P. 2001 Modeling turbulent collision of bidisperse inertial particles. *J. Fluid Mech.* **433**, 77.